Magnetization curves of antiferromagnets with several antiferromagnetism axes

K. B. Vlasov, R. I. Zaĭnullina, and M. A. Milyaev

Institute of Metal Physics, Urals Division, USSR Academy of Sciences

Results are presented of theoretical and experimental investigations (with single-crystal $FeGe_2$ as the example) of the magnetization curves of tetragonal-symmetry antiferromagnets having easy magnetization planes with preferred antiferromagnetism axes (crystallographic magnetic-anisotropy constants $K_2 < 0$ and $K_4 \neq 0$). It is shown that the crystal magnetization is determined both by intradomain processes and by displacements of the interdomain walls. The regularities due to these processes are determined.

Magnetization curves have been customarily investigated for magnetic single-axis antiferromagnets having tetragonal or lower crystal symmetry (see, e.g., Refs. 1–3). The domains into which a magnetic-uniaxial antiferromagnet is broken up by degeneracy have in a magnetic field equal energies, and the field does not lead to displacement of the domain walls. The magnetization processes take place as if the antiferromagnet were in a magnetically homogeneous (single-domain) state. There exist, however, antiferromagnets with several equivalent antiferromagnetism axes (tetragonal-symmetry antiferromagnets having an easy plane containing antiferromagnetism axes, cubic-symmetry antiferromagnets). In this case the contiguous domains in which the antiferromagnetism vectors are not collinear, are energetically nonequivalent. As a result the field will exert a pressure on the domain walls and cause their displacement, and hence an additional change of the resultant magnetization.

Magnetization processes in multiaxial antiferromagnets in a magnetically homogeneous state are considered in Refs. 4 and 5.

In the present communication we present, with single-crystal $FeGe_2$ as the example, the results of both a theoretical and an experimental investigation of the magnetization curves of antiferromagnets in which domain-wall displacements are possible.

1. THEORY

1. We investigate first the case of a magnetically homogeneous (single-domain) distribution of the sublattice magnetization vectors $\mathbf{I}^{(1)}$ and $\mathbf{I}^{(2)}$, and consequently of the antiferromagnetism $\mathbf{L} = \mathbf{I}^{(1)} - \mathbf{I}^{(2)}$ and the resultant magnetization $\mathbf{I} = \mathbf{I}^{(1)} + \mathbf{I}^{(2)}$ vectors. It will be shown below that the relations obtained in this analysis are valid for single crystals of real multidomain antiferromagnets magnetized in directions that are symmetric relative to the antiferromagnetism axes.

We consider antiferromagnets having a tetragonal crystal structure, in which the second-order crystallographic magnetic anisotropy constant is $K_2 < 0$, i.e., the vector $\mathbf{L}$ lies in the basal plane (001). We confine ourselves to cases in which the vector $\mathbf{H}$ also lies in this plane.

We introduce the angles φ and β that determine respectively the orientations of the vectors $\mathbf{L}$ and $\mathbf{H}$ relative to the [100] axis and the angle between the vectors $\mathbf{L}$ and $\mathbf{H}$, with $\varphi = \beta + \psi$. We take into account the anisotropy energy F_A in the basal plane and the energy F_H in the external magnetic field $\mathbf{H}$:

$$F_A = {}^1\!/_4 K_4 \cos 4\varphi, \tag{1}$$
$$F_H = -\mathbf{I}\mathbf{H}, \tag{2}$$
$$\mathbf{I} = \chi\mathbf{H}, \tag{3}$$
$$\chi = \chi_\parallel \cos^2 \psi + \chi_\perp \sin^2 \psi. \tag{4}$$

K_4 is the fourth-order crystallographic magnetic anisotropy constant. Account is taken here of only the anisotropy of the susceptibility with respect to $\mathbf{H}$. In the general case it is necessary to take into account also the crystallographic anisotropy which leads to a dependence of the angle ψ on φ in (4) (see, e.g., Ref. 6). For low anisotropy in the basal plane, this dependence can be neglected. In addition, we consider the region of fields considerably weaker than the effective field of the exchange interaction between the magnetic sublattices. The parallel and perpendicular susceptibilities $\chi_\parallel$ and $\chi_\perp$, just as K_4, are fundamental material constants characterizing the particular form of the antiferromagnet. They are insensitive to structure and depend only on the temperature T.

The equilibrium orientation of the antiferromagnetism vector $\mathbf{L}$ and hence also the magnetization $\mathbf{I}$ are determined from the condition that the free energy $F = F_A + F_H$ be a minimum:

$$\frac{\partial F}{\partial \varphi} = 0.$$

For $H = 0$ we obtain solutions of two types:

for $K_4 < 0$
$$\varphi_\mathrm{I} = k \cdot 90°, \quad k = 0, 1, 2, 3,$$
for $K_4 > 0$
$$\varphi_\mathrm{II} = 45° + k \cdot 90°,$$

which determine the orientations of the antiferromagnetism axes. In the first case the antiferromagnetism axes are of type [100], and in the second of type [110].

We consider cases when the magnetization is along principal crystallographic axes: $\mathbf{H} \parallel [100]$ ($\beta = 0$) and $\mathbf{H} \parallel [110]$ ($\beta = 45°$). To be specific, we put $K_4 > 0$, as is the case in $FeGe_2$. For a magnetic field applied along a direction symmetric to the antiferromagnetic axes ($\mathbf{H} \parallel [100]$) we have

$$\cos^2 \varphi = {}^1\!/_2 [1 - (H/H_0)^2], \quad H \leqslant H_0,$$
$$\varphi = 90°, 270°, \quad H \geqslant H_0.$$

From (3) and (4) we obtain for the magnetization

$$I = {}^1\!/_2 [\chi_\perp + \chi_\parallel + (\chi_\perp - \chi_\parallel)(H/H_0)^2] H, \quad H \leqslant H_0, \quad I = \chi_\perp H, \quad H \geqslant H_0 \tag{5}$$

and for the differential susceptibility

$$\chi = \tfrac{1}{2}[\chi_\perp + \chi_\| + 3(\chi_\perp - \chi_\|)(H/H_0)^2], \quad H \leqslant H_0,$$
$$\chi = \chi_\perp, \qquad\qquad\qquad\qquad\qquad H \geqslant H_0, \quad (6)$$

where

$$H_0^2 = 2K_4/(\chi_\perp - \chi_\|). \quad (7)$$

As seen from (6), χ changes jumpwise at $H = H_0$.

For a field applied along one of the antiferromagnetism axes ($H\|[110]$), for arbitrary H, we have

$$\varphi = 90°,\ 270°, \quad I = \chi_\perp H, \quad \chi = \chi_\perp, \quad (8)$$

if $L\perp H$ in the initial state $H = 0$.

If, however, $L\|H$, the following relations hold:

$$\varphi = 0,\ 180°, \quad H \leqslant H_0,$$

$$\varphi = 90,\ 270°, \quad H \geqslant H_0,$$

and hence

$$I = \chi_\| H, \quad \chi = \chi_\|, \quad H \leqslant H_0,$$
$$I = \chi_\perp H, \quad \chi = \chi_\perp, \quad H \geqslant H_0. \quad (9)$$

Relations (5)–(9) describe, firstly, the para-process ($\chi_\|$), i.e., the changes produced in the sublattice magnetization vectors by the components of the magnetic-field intensity vector along the directions of the magnetizations of the magnetic sublattices, secondly the bending of the magnetic-sublattice magnetization vectors relative to one another ($\chi_\perp$) under the influence of the magnetic-field component perpendicular to L, and thirdly the rotation of the vector L (rotation of the angle φ from H).

In the case of magnetization in a direction symmetric relative to the antiferromagnetism axes ($H\|[100]$) in the field H_0, the process of rotation of the vector L is completed. For magnetization along one of the antiferromagnetism axes ($H\|[110]$) at $H = H_0$, reversal of the sublattice magnetizations takes place if $L\|H$ in the initial state. This process should led to a first-order magnetic phase transition. If, however, $L\perp H$ in the initial state, the field H should not cause rotation of the vector L, so that no phase transition should occur.

2. We consider now real antiferromagnets with account taken of their domain structure.

We recall first some relations from the general theory that describes reversible domain-structure changes caused by external forces.[7] We denote the free energy of a domain of species in the field of external forces by $(F_e)_i$. If these energies are different in contiguous ith and kth domains, the wall between these domains is under a pressure that moves it a distance δn_{ik}. The work of this pressure should supply the increase of the bulk free energy $(F_i)_i$, due to magnetoelastic-anisotropy forces, as well as compensate for the change of the surface free energy of the walls separating domains of species i and k. A change of the external forces that lead to the change $\delta[(F_e)_k - (F_e)_i]$ causes the wall to move a distance

$$\delta n_{ik} = C_{ik}\delta[(F_e)_k - (F_e)_i], \quad (10)$$

$$\frac{1}{C_{ik}} = \frac{\partial[(F_i)_i - (F_i)_k + \partial\gamma_{ik}/\partial n_{ik} + \gamma_{ik}(1/R_1 + 1/R_2)_{ik}]}{\partial n_{ik}}$$

$$+ \gamma_{ik}\frac{\partial^2 \ln S_{ik}}{\partial n_{ik}^2}, \quad (11)$$

where γ_{ik} is the density of the surface free energy, S_{ik} the surface area of the walls between the domains of species i and k per unit volume, and $R_{1,2}$ are the principal curvature radii of the walls.

The first term is due firstly to inhomogeneity of the difference of the internal energies of the contiguous walls, which results from the presence of external stresses, secondly to the inhomogeneity of the surface-energy density, and thirdly to the inhomogeneity of the change produced in the wall surface area S_{ik} by the change of its curvature (the Laplace stress). The second term is due to the change of the wall surface area S_{ik}, resulting from the deformation of the wall contour. This term must be taken into account for magnetic materials that contain, for example, nonmagnetic inclusions.

Wall displacements lead to a change of the density n_i of the magnetic phase (meaning the relative volume occupied by the domains of species i) due to the change of the volume of the neighboring phases:

$$\delta n_i = \sum_{k(\neq i)} \delta n_{ik} S_{ik}. \quad (12)$$

Assuming next that the domain-wall area is

$$S_{ik} = \varepsilon_{ik} n_i n_k, \quad (13)$$

we have (see Ref. 7) with allowance for (12) and (13)

$$n_i = \frac{\exp\{-C_{ik}\varepsilon_{ik}[(F_e)_i - a_i]\}}{\sum_k \exp\{-C_{ik}\varepsilon_{ik}[(F_e)_k - a_k]\}}, \quad (14)$$

where a_i are integration constants.

We proceed now to describe the antiferromagnets considered in Sec. 1 when they contain a domain structure. The degenerate states in these antiferromagnets are those in which the vectors L are mutually antiparallel, and also the states in which the vectors L are mutually perpendicular. Two domain types, separated by 180-degree and 90-degree walls, are thus possible.

In investigations of the influence of H on ferromagnets, the energy $(F_e)_i$ of a domain of species i must be taken to mean its energy $(F_H)_i$ in the field H

$$(F_H)_i = -I_i H, \quad I_i = \chi_i H,$$
$$\chi_i = \chi_\| \cos^2 \psi_i + \chi_\perp \sin^2 \psi_i. \quad (15)$$

If the contiguous i and k domains are separated by a 180-degree wall, their angles are $\psi_k = \psi_i + 180°$. According to (15), $\chi_i = \chi_k$ and $(F_H)_i = (F_H)_k$. The field H will exert no pressure on the walls between these domains, and according to (10) no displacement of 180-degree walls will take place. These domains behave equivalently in a magnetic field. There will be produced in them equal magnetization changes due to the para process, to the bending of the magnetic sublattices, and to the rotation process, as if the antiferromagnet were magnetically homogeneous. We shall therefore regard domains of this type as being of the same species.

The domains of the second type, separated by 90-degree walls, can be divided into two species. In these domains the orientations of the vectors L relative to the magnetic field, given by the angles ψ_1 and ψ_2, are different. The domain energies in a magnetic field are therefore also different. We

170   Sov. Phys. JETP 72 (1), January 1991

Vlasov et al.   170

can consider accordingly to species of magnetic phases, characterized by magnetizations $I_{1,2}$ (15) and densities $n_{1,2}$, $n_1 + n_2 = 1$. We put $n_2 = n$, so that $n_1 = 1 - n$. The resultant change of the magnetization is determined by two terms

$$\delta I = \delta I_{id} + \delta I_{wd}, \tag{16}$$

where

$$\delta I_{id} = (1-n)\delta I_1 + n\delta I_2 \tag{17}$$

describes intradomain processes, and

$$\delta I_{wd} = (I_2 - I_1)S_{12}\delta n_{12} \tag{18}$$

describes wall-displacement processes.

Taking (10),(15),(17), and (18) into account we obtain for the differential reversible susceptibility χ of the multidomain state the relations

$$\chi = \chi_{id} + \chi_{wd} \tag{19}$$

$$\chi_{id} = (1-n)\chi_1 + n\chi_2 + \left[(1-n)\frac{\partial\chi_1}{\partial H} + n\frac{\partial\chi_2}{\partial H} \right] H, \tag{20}$$

$$\chi_{wd} = \left[2(\chi_2 - \chi_1) + \frac{\partial(\chi_2 - \chi_1)}{\partial H}H \right](H/H^*)^2(1-n)n, \tag{21}$$

where

$$n = \{1 + \exp[-[(H/H^*)^2 - a]]\}^{-1},$$
$$(1-n)n = \tfrac{1}{2}\{1 + \text{ch}[(H/H^*)^2 - a]\}^{-1}, \tag{22}$$

$$(H^*)^2 = \{C_{12}\varepsilon_{12}(\chi_2 - \chi_1)\}^{-1}, \tag{23}$$

a is an integration constant and determines the initial density n^0 of the magnetic phases at $H = 0$.

In the general case of arbitrary orientation of $\mathbf{H}$ the angles ψ_1 and ψ_2, and hence according to (15) and (23), χ_1, χ_2 and H^*, depend on $\mathbf{H}$. This dependence is due to rotation of the vector $\mathbf{L}$ by the field $\mathbf{H}$ and is determined by the minimum of the free energy.

The situation is considerably simplified when wall displacements and rotations can be disregarded.

The former situation arises in the case of magnetization in crystallographic directions, in which the antiferromagnetism vectors of contiguous domains are symmetrically oriented about the field $\mathbf{H}$.

The latter situation occurs for magnetization in crystallographic directions in which no rotation of the vectors $\mathbf{L}$ occurs in a certain range of fields, while $\chi_1 = \chi_1^0$ and $\chi_2 = \chi_2^0$. The equations obtained for the second case are valid, with good approximation, also for arbitrary orientation of $\mathbf{H}$ relative to the crystallographic axes if $H^* \ll H_0$, i.e., if rotation processes can be neglected.

We consider tetragonal-symmetry antiferromagnets with $K_4 > 0$. Domains of species $i = 1$ are taken to be domains with angles $\varphi_1^0 = 45° + k\cdot180°$, at $H = 0$, and those of species $i = 2$ have $\varphi_2^0 = -45° = k\cdot180°(k = 0, 1)$.

The first case is realized when the magnetic field is applied in a direction symmetric relative to the antiferromagnetism axes $(\mathbf{H})\|[100])$. In this case $\psi_1 = \psi_2 = \psi$ and according to (20) and (21) we have

$$\chi_{wd} = 0,$$

$$\chi_{id} = (1-n)\chi_1 + n\chi_2 = \chi_\| \cos^2\psi + \chi_\perp \sin^2\psi.$$

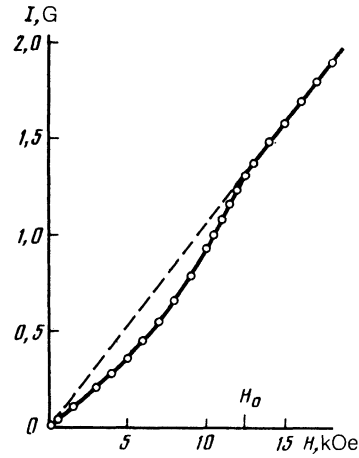The relations for χ_{id} no longer contain the densities of the

FIG. 1. Magnetization curve of $FeGe_2$ crystal at $\mathbf{H}\|[100]$ and $T = 77$ K. Solid curve—calculation on the basis of Eq. (5), circles—experiment.

magnetic phases. They coincide with expression (4). The equilibrium orientations of the vectors $\mathbf{L}_1$ and $\mathbf{L}_2$, which are specified by the angle ψ, are obtained from the condition that the free energy $F = F_A + F_H$ be a minimum. The $I(H)$ and $\chi(H)$ dependences have the same form as for the single-domain state [see Eqs. (5) and (6) and Figs. 1 and 2 (calculated curves)]. Evidently, a second order phase transition should be observed in this case at $H = H_0$.

Since the field $\mathbf{H}$ does not lift the degeneracy of either the first or the second type, an antiferromagnet magnetized in fields $H > H_0$ remains in a single-domain state in which not only 180-degree but also 90-degree neighborhoods are preserved.

The second case is realized when the magnetic field $\mathbf{H}$ is applied along one of the antiferromagnetism axes $(\mathbf{H}\|[110])$. The orientation of the vector $\mathbf{L}_2$ does not change in the course of magnetization, since $\mathbf{L}_2 \perp \mathbf{H}$. According to (9), the direction of the vector $\mathbf{L}_1$ does not change in a field $H < H_0$. The angles ψ_1 and ψ_2 are thus equal to their values at $H = 0$: $\psi_1^0 = 0$, $\psi_2^0 = 90°$ and, according to (15), $\chi_1 = \chi_\|$, $\chi_2 = \chi_\perp$, $n = n_1$, where n_1 is the density of the magnetic phase with $\mathbf{L} \perp \mathbf{H}$. From (20)–(23) we have

$$\chi_{id} = \chi_\|\{1 + \exp[(H/H^*)^2 - a]\}^{-1}$$
$$+ \chi_\perp\{1 + \exp[-[(H/H^*)^2 - a]]\}^{-1}, \tag{24}$$
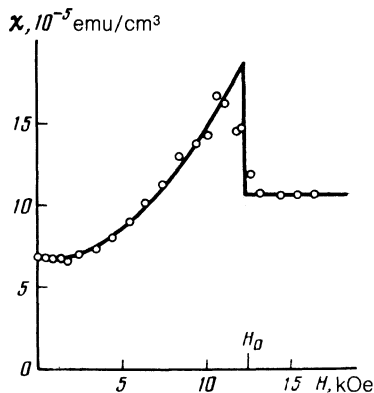

FIG. 2. Dependence of the differential susceptibility on H at $\mathbf{H}\|[100]$, $T = 77$ K. Solid curve—calculation on the basis of Eq. (6), circles—experiment.

$$\chi_{wd}|=(\chi_\perp-\chi_\parallel)\ (H/H^*)^2\{1+\mathrm{ch}\ [(H/H^*)^2-a]\}^{-1}, \qquad (25)$$

$$(H^*)^2=[C_{12}\varepsilon_{12}(\chi_\perp-\chi_\parallel)]^{-1}. \qquad (26)$$

According to (13), the constant ε_{12} can be determined from the area S^0_{12} of the 90-degree walls between the domains in the initial magnetic state (at $H=0$):

$$\varepsilon_{12}=S_{12}{}^0/n_\perp{}^0(1-n_\perp{}^0). \qquad (27)$$

The field H^*, in contrast to H_0, is sensitive to the magnetic and crystal structures. It is determined, according to (26), (27), and (11), by the initial density $n^0_\perp$ of the magnetic field, the initial area S^0_{12} of the interdomain walls, and by the inhomogeneities of the crystal (internal stresses, densities of foreign impurities and alloy components, foreign inclusions etc.) which cause F_i and γ_{12} to be inhomogeneous.

Figure 3 (curves 1, 2, and 3) shows the dependences of χ, χ_{id}, and χ_{wd} on H, plotted in accordance with (24) and (25). It is clearly seen from the equations and from the curves that the reversible displacement processes are most intense in the vicinity of the field H^*. Their fraction in the resultant susceptibility decreases to zero, both as $H\to0$ (in contrast to the situation for magnetically soft ferromagnets) and at $H\gg H^*$. Intradomain processes play a substantial role both as $H\to0$ (in contrast to magnetically soft ferromagnets) and at $H\gg H^*$. Namely, χ_{id} increases monotonically from a value $(\chi_\perp-\chi_\parallel)n^0_\perp+\chi_\parallel$ at $H=0$ to a value $\chi_\perp$ at $H\gg H^*$. Although the magnetic field does not eliminate the domain structure completely at $H\gg H^*$ (domains separated by 180-degree walls remain), the magnetization and magnetic susceptibility in fields $H\gg H_0$ will be the same as for the case of the homogeneous state $\chi=\chi_\perp$. As seen from Eqs. (24) and (25) and from Fig. 3, the $\chi(H)$ dependences are smooth. No phase transitions of first or second order occur when H is varied. The first-order phase transition at $H=H_0$, which follows from (9), does not occur at $\mathbf{L}\perp\mathbf{H}$ because in fields $H^*<H<H_0$ the domains in which $\mathbf{L}$ is parallel or antiparallel to $\mathbf{H}$ are absorbed by the domains in which $\mathbf{L}\perp\mathbf{H}$.

Irreversible wall displacements should occur in addition to the reversible ones. They lead to an additional term χ^{ir}_{wd} (irreversible susceptibility due to wall displacements)

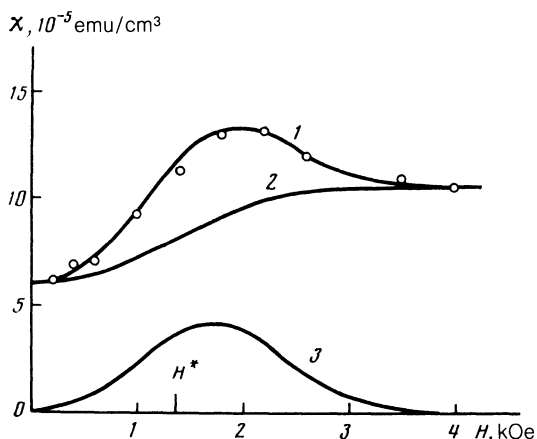FIG. 3. Field dependences of the differential reversible susceptibility at $\mathbf{H}\|[110]$ (curve 1) and of its components χ_{id} (curve 2) and χ_{wd} (curve 3) at $T=77$ K. Solid curves—calculation based on Eqs. (19)–(21), circles—experiment.

in the expression for the differential susceptibility, and to the following effects: first, to hysteresis and second, to an influence of magnetic annealing on the form of the magnetization curves $I(H)$.

An antiferromagnet cooled from temperatures above the Néel point T_N to a certain $T(T<T_N)$ breaks up into domains. When a field is applied along one of the antiferromagnetism axes (the [110] axis) its magnetization varies along the pristine magnetization curve up to fields $(H\gg H^*)$ in which the displacements of the 90-degree walls terminate. If this is followed by a decrease of the magnetic field from the value $H\gg H^*$, multidomain states with 90-degree neighborhoods may not occur at all, or states may occur with magnetic-field distribution entirely different than those for increasing H. As a result, when H is lowered to zero the descending branch of the plot of I vs H, while passing through the point $H=0, I=0$, will not coincide with the pristine curve (it will lie "lower"). This can lead to the onset of a closed loop when the field is cyclically varied between 0 and H. The slopes of the tangents to the ascending and descending branches of the $I(H)$ curve should be equal because the densities $n^0_\perp$ are equal in this case.

The cause of the influence of magnetic annealing on the shape of the $I(H)$ curve is that the initial density $n^0_\perp$ of a sample cooled in a magnetic field differs from the initial density of the magnetic phase of a sample cooled in a zero field. The $I(H)$ curve of a sample cooled in a magnetic field from temperatures $T>T_N$ should lie "higher" (be less concave) than the $I(H)$ curve cooled to in a zero field.

We note finally that all the equations and their conclusions for the investigated cases are valid also for tetragonal antiferromagnets having an easy plane at $K_4<0$. The situation for $\mathbf{H}\|[100]$ and $K_4<0$, turns out to be the same as for $\mathbf{H}\|[110]$ and $K_4>0$. A similar picture should be observed also for antiferromagnets having cubic symmetry, in which the antiferromagnetism axes are of the type [100] and the field $\mathbf{H}$ lies in a cubic face.

2. EXPERIMENT

We investigated iron digermanide $FeGe_2$ (space group $I4/mcm$). It is subject to two magnetostructural phase transitions: of first order at $T_1=265$ K and of second order at $T_2=287$ K. According to neutron-diffraction data[8] the sequence of the magnetic structures in $FeGe_2$ is the following: paramagnetism $(T>T_2)$—incommensurate structure $(T_1<T<T_2)$—collinear antiferromagnetic structure $(T<T_1)$. The antiferromagnetism axes in the easy plane (001) are of the type $[110](K_2<0, K_4>0)$.

The magnetization curves of single-crystal $FeGe_2$ in fields up to 18 kOe were measured with a vibrating-reed magnetometer. The mean squared deviation of the measurement results did not exceed 0.1%. The specified temperature was maintained accurate to within 0.1 K.

Figure 1 shows the magnetization curve $I(H)$ of single-crystal $FeGe_2$ plotted at $T=77$ K with a field applied along a direction symmetric about the antiferromagnetism axes ($\mathbf{H}\|[100]$). The experimental data are marked by points, and the curve is plotted in accordance with Eq. (5). The value of H_0 was determined by least squares.

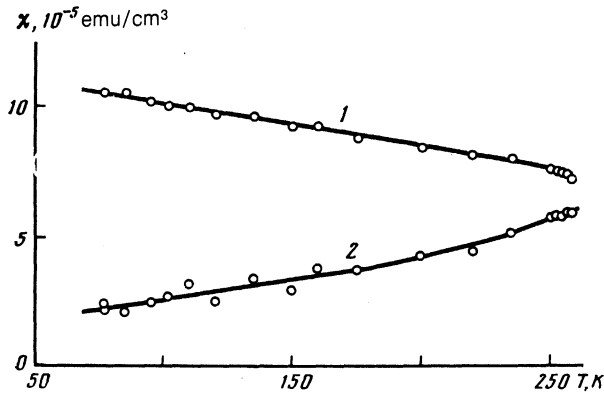Figure 2 shows the differential-susceptibility curve calculated from Eqs. (6); the points mark the susceptibilities

χ, 10^{-5} emu/cm^3

FIG. 4. Temperature dependences of the perpendicular ($\chi_\perp$, curve 1) and parallel ($\chi_\parallel$, curve 2) susceptibilities of single-crystal FeGe$_2$.

K_4, 10^{-3} erg/cm^3

FIG. 6. Temperature dependence of the crystallographic-magnetic-susceptibility constant K_4 of FeGe$_2$.

obtained by differentiating the experimental $I(H)$ curve. The $I(H)$ and $\chi(H)$ curves are reversible, namely, they turn out to be the same for both an increasing and a decreasing field H, as well as after cooling in a field H from temperatures $T > T_2$. A second-order phase transition is observed in a field $H = H_0$. Measurements at different temperatures have shown that higher temperatures correspond to less concave $I(H)$ curves. The good agreement between the experimental data and the theoretical curves indicates that magnetization in a direction symmetric relative to the antiferromagnetism axes ($\mathbf{H}\|[100]$), is due only to intradomain processes. The reason for absence of hysteresis and of an influence of magnetic annealing is that no wall displacements occur at the field orientation in question.

As seen from the arguments above, it is possible to determine from the magnetization curves at $\mathbf{H}\|[100]$ the material constants $\chi_\perp$, $\chi_\parallel$ and K_4. The value of $\chi_\perp$ is determined from the value of χ at $H > H_0$. $\chi_\parallel$ is determined from the value of χ measured as $H \to 0$ and equal to $\chi = \frac{1}{2}(\chi_\perp + \chi_\parallel)$. Our measurements of $I(H)$ at various temperatures made it possible to obtain the temperature dependences of $H_0(T)$, $\chi_\perp(T)$, $\chi_\parallel(T)$, and also the temperature dependence of the anisotropy constant K_4 calculated from Eq. 7. Figures 4–6 show the $\chi_\perp(T)$, $\chi_\parallel(T)$, $H_0(T)$ and $K_4(T)$ dependences. It follows from these figures that as $T \to T_1$ the difference $\chi_\perp - \chi_\parallel$ does not vanish, whereas H_0 and K_4 tend to zero. It can be assumed that the magnetostructural first-order phase
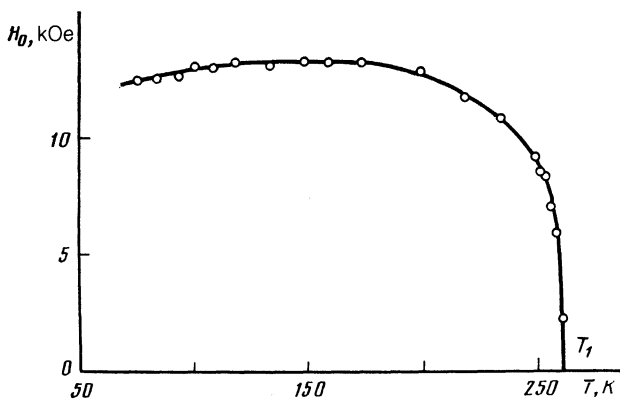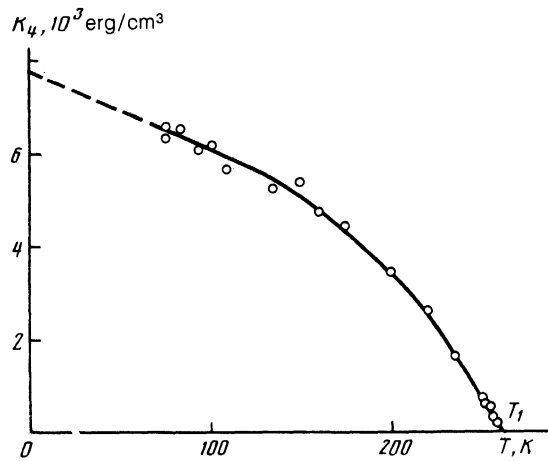

FIG. 5. Temperature dependence of the field H_0.

transition at T_1 in FeGe$_2$ is due to a reversal of the sign of the crystallographic magnetic anisotropy K_4.

Let us consider the magnetization curves and the susceptibilities following application of a field along one of the antiferromagnetism axes ($\mathbf{H}\|[110]$). Magnetization along this axis produces both reversible and irreversible wall displacements.

Figure 3 shows plots of the reversible differential susceptibility χ and of its terms χ_{wd} and χ_{id} against H. The experimental values of $\chi(H)$ are shown by the points on curve 1 of Fig. 3. The values of χ were defined as the ratios $\Delta I / \Delta H$ for a field decreasing from H to $H - \Delta H$ ($\Delta H = 30$ Oe). Before measuring χ in each specified, field, the sample was heated to $T = 300$ K ($T > T_2$), kept for 0.5 h at this temperature, and then cooled in a zero field to the measurement temperature. The good agreement between the experimental data and the theoretical curve and the agreement with the theoretical deductions indicate that for magnetization along this axis the variations of the magnetization and susceptibility with the field are determined both by intradomain processes (paraprocess with bending of the magnetization sublattices, but in the absence of rotation) and by displacements of the domain walls.

Measurements of $\chi(H)$ at various temperatures yielded plots of $n_\perp^0(T)$ and $H^*(T)$ (curve 1, Fig. 7) obtained from the relations (22), (24) and (25). As expected, $n_\perp^0 = 0.5$ for all temperatures $T < T_1$.

Analysis of the form of $H^*(T)$ plot, based on Eqs. (26), (27), and (11), suggests the following probable mechanism that slows down the domain-wall displacements.

Note (see, e.g., Ref. 9) that $F_i \sim \lambda\sigma_i$, $\gamma \sim [(K_4 + \lambda\sigma_i)A]^{1/2}$. The exchange interaction constant $A \sim (I_s/I_0)^2$, where I_s and I_0 are respectively the sublattice magnetizations at T and $T = 0$, λ is the magnetostriction in the basal plane, and σ_i are the internal stresses. If the stresses are due to the existence of 90-degree neighborhoods of domains, then $\sigma_i = E\lambda$, where E is the elastic modulus. At $T = 77$ K, FeGe$_2$ has $K_4 \sim 10^4$ erg/cm^3, $\lambda \sim 10^{-5}$, and $E \sim 10^{12}$ dyn/cm^2, whence $\lambda\sigma_i \sim 10^2$ erg/cm^3, with $K_4 \gg \lambda\sigma_i$ in a wide temperature range.

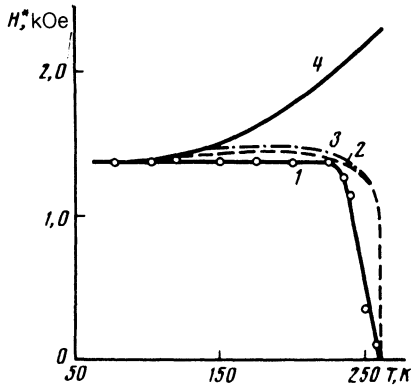Assume that the inhomogeneity of F_i and γ is due to inhomogeneity of σ_i. Then

FIG. 7. Temperature dependence of H^* (curve 1). Calculated temperature dependences of the terms of $H^*(T)$ for wall-displacement energy is due to: inhomogeneity of the magnetoelastic energy (H_1^*, curve 2), change of domain-wall area (H_3^*, curve 3), and inhomogeneity of γ, (H_2^*, curve 4). The initial values of H^* are made to coincide at $T = 77$ K.

$$\frac{\partial F_i}{\partial n} \sim \lambda \frac{\partial \sigma_i}{\partial n} \quad \frac{\partial \gamma}{\partial n} \sim \frac{A\lambda}{\gamma} \frac{\partial \sigma_i}{\partial n} \quad \frac{\partial^2 \gamma}{\partial n^2} \sim \frac{A\lambda}{\gamma} \frac{\partial^2 \sigma_i}{\partial n^2}.$$

It was recognized in the calculation of $\partial^2\gamma/\partial n^2$ that σ_i is in a state in which γ is a minimum. In this case we get, according to (26) and (11)

$$H^{*2} = H_1^{*2} + H_2^{*2} + H_3^{*2}.$$

The term $H_1^* \sim [\lambda/(\chi_\perp - \chi_\parallel)]^{1/2}$ is due to the inhomogeneity of the magnetoelastic energy, the term $H_2^* \sim [A\lambda/\gamma(\chi_\perp - \chi_\parallel)]^{1/2}$ to inhomogeneity of γ, and the term $H_3^* \sim [\gamma/(\chi_\perp - \chi_\parallel)]^{1/2}$ to the variation of the wall areas. The temperature dependences of these terms are shown in Fig. 7 (curves 2–4). The $\lambda(T)$ was taken from Ref. 10, and $I_s/I_0(T)$ was determined using the Brillouin function. The starting points of the $H_1^*(T)$, $H_2^*(T)$ and $H_3^*(T)$ curves coincide with the experimental $H^*(T)$ curve at $T = 77$ K. The temperature dependences of $H_1^*(T)$ and $H_3^*(T)$ are closest to the experimental $H^*(T)$. The most probable cause of the slower motion of domain walls can be the inhomogeneity of the magnetoelastic energy as well as the inhomogeneity of the domain-wall area.

The term χ_{wd}^{ir}, due to irreversible wall displacements, in the differential magnetic susceptibility tends to zero for $H \to 0$ and $H \gg H^*$. In a field $H = H^*$ the susceptibility χ_{wd}^{ir} is 20% of the reversible differential susceptibility χ.

Figure 8 shows $I(H)$ magnetization curves plotted at $T = 77$ K. It can be seen that in fields $H < 2.5$ kOe, i.e., $H \ll H_0$ ($H_0 = 12.5$ kOe). The $I(H)$ dependences are nonlinear, and go over at $H \gg H^*$ into a linear dependence that coincides with the linear $I(H)$ obtained for the case $H \parallel [100]$ and extrapolated to a field $H = 0$. Curve 1 corresponds to the pristine magnetization curve. When the field decreases from a certain value $H(H \gg H^*)$ to zero, the descending branch of the $I(H)$ curve (curve 2) lies above the pristine curve in the first cycle. Identical closed $I(H)$ loops are produced in all the succeeding cycles of increasing (curve 3) and decreasing H (again curve 2). In accord with the prediction of the theory, the slopes of the tangents to the ascending and descending branches of the loop turned out to be equal. The density of the magnetic phase is in this case
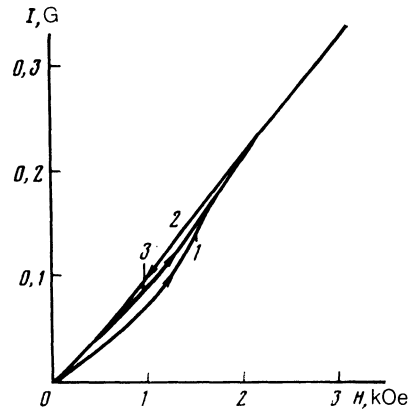

FIG. 8. Magnetization curves of single-crystal $FeGe_2$ for the case $H \parallel [110]$ at $T = 77$ K, 1—pristine magnetization curve, 3 and 2—hysteresis loop.

$n_1^{res} = 0.82$. Note that the density $n_1^{res} - n_1^0$ plays a role similar to that of the residual magnetization of ferromagnets.

Reversal of the magnetization (change of the field from $+H$ to $-H$) produces a drawn-out hysteresis loop ($I = 0$ at $H = 0$), the two lobes of which in the quadrants $H > 0$, $I > 0$ and $H < 0$, $I < 0$, are the cyclic loops considered above and obtained in the field range from 0 to H.

Note that, unlike in ferromagnets, the pristine magnetization curve (curve 1) is outside the hysteresis loop. The reason is that the density $n_\perp$ of the magnetic phase with $L \perp H$ is higher on the hysteresis loops than the density of this phase on the pristine curve for identical values of H, including $H = 0$, when $n_1^{res} > n_1^0$ and $I = 0$.

As was indeed assumed, the magnetization curve plotted after magnetic annealing (cooling in a field $H = 10$ kOe from $T > T_2$ to $T = 77$ K) lies "higher" than the pristine (less concave) curve. The magnetic phase with $L \perp H$ at $H = 0$($n_1^0 = 0.86$) is higher than the density of the same phase of a sample cooled in a zero field.

Note finally that it follows from the forms of $\chi(H)$ (Fig. 3, curve 1) and $I(H)$ (Fig. 8) that magnetization along one of the antiferromagnet axes produces neither first-nor second-order magnetic phase transitions.

3. CONCLUSION

Magnetization in tetragonal- and cubic-symmetry antiferromagnetic crystals having several antiferromagnetism axes is determined in the general case by both intradomain processes (the paraprocess, bending of the sublattice magnetizations relative to one another, rotation of the antiferromagnetism vector, characterized by susceptibilities $\chi_\parallel$ and $\chi_\perp$ and by an anisotropy constant K_4), as well as by displacement of the domain walls.

Magnetization along a direction symmetric about the antiferromagnetism axes is determined only by intradomain processes. The magnetization curves $I(H)$ are characterized by the difference ($\chi_\perp - \chi_\parallel$) and by a structurally insensitive field $H_0^2 = 2K_4/(\chi_\perp - \chi_\parallel)$. When this field is increased with increase of H, the rotation stops, the nonlinear character of $I(H)$ gives way to the linear $I = \chi_\perp H$, and a second-order phase transition is produced.

The magnetization along one of the antiferromagnetism axes is determined by intradomain processes (with the ex-

ception of rotation) as well as by displacement of the domain walls. The displacement is most intense in fields close to H^*. It makes a zero contribution to the magnetic susceptibility χ not only in strong fields ($H \gg H^*$) but also as $H \to 0$. Intradomain processes play a substantial role not only at $H \gg H^*$ but also as $H \to 0$, and their contribution to χ increases with increase of H. The transition from a nonlinear $I(H)$ dependence to the linear $I = \chi_\perp H$ at $H \gg H^*$ is smooth and neither first- nor second-order transitions occur. The field H^* is a structurally sensitive property. It is determined by the initial magnetic-phase density, by the initial area of the interdomain walls, and also by the crystal inhomogeneities that determine the inhomogeneity of the magnetoelastic energy and of the surface energy of the domain walls. Owing to the irreversible character of the magnetization process, hysteresis is possible in this case, and magnetic annealing influence substantially the shapes of the $I(H)$ and $\chi(H)$ curves.

The value of $\chi_\perp - \chi_\parallel$ in $FeGe_2$ decreases with increase of T, but does not vanish at $T = T_1$, whereas H_0 and K_4 vanish at $T = T_1$. It appears that the magnetostructural first-order transition at T_1 is due to the reversal of the sign of K_4 with change of T.

It follows from analysis of the $H^*(T)$ curves that the most probable causes of the slower displacements of the domain walls are inhomogeneities of the magnetoelastic energy and of the domain-wall area.

[1] A. S. Borovik-Romanov, *Antiferromagnetism* [in Russian], Itogi Nauki [Science Summaries], AN SSSR (1963), Chap. 3.

[2] E. A. Turov, *Physical Properties of Magnetically Ordered Crystals* [in Russian], AN SSSR (1963), Chap. 4.

[3] S. V. Vonsovskii, *Magnetism*, Halsted, 1975, Ch. 22, pp. 5–6.

[4] W. J. Ince, J. Appl. Phys. **37**, 1132 (1966).

[5] A. G. Berezin and V. G. Shavrov, Zh. Eksp. Teor. Fiz. **71**, 2362 (1966) [Sov. Phys. JETP **75**, 1242 (1977)].

[6] K. B. Vlasov, Izv. AN SSSR, ser. fiz. **18**, 339 (1954).

[7] S. V. Vonsovskiĭ and Ya. S. Shur, *Ferromagnetism* [in Russian], Gostekhizdat (1984), Ch. 7, pp. 53–56.

[8] L. M. Corliss, J. M. Hastings, W. Kinmann *et al.*, Phys. Rev. B **31**, 4337 (1985).

[9] M. M. Farztdinov, *Physics of Magnetic Domains in Antiferromagnets and Ferrites* [in Russian], Nauka (1981), p. 25.

[10] E. Franus-Muir, E. Fawcett, and V. Pluzhnikov, Sol. St. Commun. **52**, 615 (1984).

Translated by J. G. Adashko